Acta Cryst. (1979). A**35**, 895–900

Determination of Crystal Structure Factors of Si by the Intersecting-Kikuchi-Line Method

By O. Terasaki and D. Watanabe

Department of Physics, Faculty of Science, Tohoku University, Aramaki-Aoba, Sendai 980, *Japan*

and J. Gjønnes

Department of Physics, University of Oslo, Blindern, Oslo 3, *Norway*

(*Received* 19 *February* 1979; *accepted* 9 *May* 1979)

Abstract

The intersecting-Kikuchi-line method, which is one of the electron diffraction methods of determining crystal structure factors, has been applied to Si at 1000 kV, with the object of improving the accuracy. It is shown that, with a favourable choice of line intersections, the accuracy is improved by at least a factor of two at 1000 kV compared to the case of 100 kV. From the intersections of the weak Kikuchi lines 1004, $9\bar{1}3$ and 0106 with the $\bar{1}\bar{1}\bar{1}$ line and from those of the $9\bar{1}3$, $8\bar{2}2$ and $\bar{1}95$ lines with the $\bar{2}\bar{2}\bar{2}$ line, both the 111 and 222 structure factors are determined simultaneously, including their sign. The 220 structure factor, which cannot be determined by the critical-voltage method unless an accelerating voltage higher than 1000 kV is applied, is also determined from the intersection of the $95\bar{3}$ line with the $\bar{2}\bar{2}0$ line. The results obtained agree with those determined by the X-ray *Pendellösung* method.

1. Introduction

The development of precise electron diffraction methods for the determination of structure factors has received considerable attention in recent years and considerable advances have been made; for a review see Goodman (1978). Methods which are based upon special effects in Kikuchi patterns seem to offer several advantages: no special crystal shape is needed, and the measurement is focussed upon distinct and very sensitive features, whereby quite high accuracy has been attained, notably in the critical-voltage method (Watanabe, Uyeda & Fukuhara, 1968, 1969). There are also, however, disadvantages which are apparent in this method. It can be applied if a mass ratio

$$m/m_o \sim U_{2h}\, h^2/(U_h^2 - U_{2h}^2) \sim U_{2h}\, h^2/U_h^2 \qquad (1)$$

can be obtained, *i.e.* when the first-order structure factor U_h is large and/or the reciprocal-lattice vector **h** is short. Thus only a few inner reflexions can be determined only when the second-order structure factor U_{2h} is known. On the other hand, the intersecting-Kikuchi-line (IKL) method, which was suggested by Gjønnes & Høier (1971) and successfully applied to disordered vanadium monoxide crystals (Høier & Andersson, 1974; Watanabe, Andersson, Gjønnes & Terasaki, 1974), is relatively independent of other structure factors. The separation between the two split segments of a Kikuchi line is measured at the intersection with a strong band, and the structure factor of the strong reflexion is determined from this separation with an accuracy of about 2% at 100 kV.

Although the accuracy of the IKL method may thus be distinctly poorer than that of the critical-voltage method, it seems to offer a useful supplement or alternative. We have therefore extended the study of the IKL method to higher voltages, in order to see whether the accuracy can be improved, while maintaining the specific advantages of the method, especially the relative independence of other structure factors. The method was applied to Si at 1000 kV and the 111, 222 and 220 structure factors were determined.

2. Principle and accuracy of the IKL method

The principle of the IKL method can be explained qualitatively by the four-beam approximation shown in Fig. 1(*a*), where point T is a projection of a Laue point on to the plane containing the reciprocal-lattice points 1, 2, 3 and 4, and the structure factors corresponding to the 1–2, 1–3, 1–4 and 4–3 couplings are U_{g-m}, $U_{g+h} = U_m$, U_g and U_h. The corresponding Kikuchi-line pattern is shown schematically in Fig. 1(*b*), where $(\mathbf{g},\bar{\mathbf{h}})$ and $(\mathbf{g}+\mathbf{h},\mathbf{h})$ are the intersections to be measured and the structure factor of the strong **h** reflexion, U_h, is to be measured. If we introduce a parameter defined by

$$\zeta = (\overline{T4})^2 - (\overline{T1})^2$$

0567-7394/79/060895-06$01.00 © 1979 International Union of Crystallography

along the broken line through T, the four eigenvalues are given by the following equations as a function of ζ (Fukuhara, 1966);

$$x^{(\alpha,\beta)} = \tfrac{1}{2}\{\zeta + U_h + U_{g-m} \pm [(\zeta + U_{g-m} - U_h)^2 + 4(U_g + U_m)^2]^{1/2}\},$$
$$x^{(\lambda,\nu)} = \tfrac{1}{2}\{\zeta - U_h - U_{g-m} \pm [(\zeta - U_{g-m} + U_h)^2 + 4(U_g - U_m)^2]^{1/2}\}. \quad (2)$$

The dispersion surface is shown in Fig. 1(*c*), where two horizontal lines denoted by $x^{(i)}$ and $x^{(j)}$ correspond to the two branches of the dispersion surface due to the 4–3 coupling with the structure factor U_h. For $\zeta = \pm(U_h - U_{g-m})$, the gaps $x^{(\alpha)} - x^{(\beta)}$ and $x^{(\lambda)} - x^{(\nu)}$ have minima, which correspond to the positions of line segments of the weak Kikuchi line **g** or **g** + **h** split along the strong $\bar{\mathbf{h}}$ or **h** line. Therefore, the separation of split segments is mainly given by $2U_h$. For the intersection of a weak Kikuchi line **g** with the second-order Kikuchi line of the strong $\bar{\mathbf{h}}$, however, three-beam interactions, **g**, **g** + **h** and **g** + 2**h**, become important to the separation of split segments. This is particularly so for the intersection with the 222 line of Si, because $|U_h| \gg |U_{2h}|$.

The accuracy of the measurement is given by the ratio of the line width to the separation of two split segments. The separation, D, as measured across the lines, is given by

$$D \sim U_h/2g, \quad (3)$$

whereas the combined effect of the widths, δ_1 and δ_2, of the two segments is $\delta = (\delta_1^2 + \delta_2^2)^{1/2} \sim (U_g^2 + U_{g+h}^2)^{1/2}/2g$ in the non-absorbing case. Finite crystal thickness or absorption will increase the line width, so will bending of the crystal, lack of proper focus, *etc.*, and δ may be written as

$$\delta \sim (U_g^2 + U_{g+h}^2 + W^2 + k^2 g^2 \varepsilon^2)^{1/2}/2g, \quad (4)$$

where W depends upon absorption and ε is an effective angular spread. Then, a resolution index can be written as

$$\delta/D \sim (U_g^2 + U_{g+h}^2 + W^2 + k^2 g^2 \varepsilon^2)^{1/2}/U_h. \quad (5)$$

Increased voltage means that W is decreased, relative to U_g and U_{g+h}, and we can then utilize intersections with larger **g** (*i.e.* smaller U_g and U_{g+h}) and thus reduce the width, provided ε is kept small. However, increased voltage also means increased many-beam interactions which may give absorption-like effects on the width. The application of the IKL method at higher voltage thus depends upon the careful selection of good intersections.

3. Experimental results

(110) Si crystals of high purity, which were thinned in a CP-4A solution, were used. Kikuchi-line patterns were obtained with selected-area diffraction using a 1000 kV electron microscope, and the accelerating voltage was measured by Høier's (1969) method as 1023 ± 2 kV.

For the determination of 111 and 222 structure factors, intersections in several projections including the 111 systematic row (Fig. 2) were investigated. [12$\bar{3}$], [23$\bar{5}$] and [15$\bar{6}$] may be typical of one quite dense, one intermediate and one very open projection. It was found that all the intersections in the [12$\bar{3}$] projection show quite strong multiple-beam interactions and rather diffuse Kikuchi-line segments. In the [23$\bar{5}$] and [15$\bar{6}$] projections, these interactions are apparent only for the closest intersections, nearest to the zone axis. [23$\bar{5}$] was chosen, however, because the intersections (**g**, $\bar{\mathbf{h}}$) show quite sharp line segments well separated from other sets of intersections (**g**+**h**, $\bar{\mathbf{h}}$), (**g**+2**h**, $\bar{\mathbf{h}}$), *etc.*

Three diffraction patterns of this projection were selected and two intersections (**g**, $\bar{\mathbf{h}}$) with the $\bar{1}\bar{1}\bar{1}$ and $\bar{2}\bar{2}\bar{2}$ lines were measured on each pattern. An example of the diffraction patterns is shown in Fig. 3. Separations were measured across the line segments (along the arrows), in order to minimize the error due to misalignment of the direction to be measured and also to avoid certain disturbing features at the band edge which are rarely discerned on the plate but will affect the calculated separation along the band edge. For the measurements, 20 enlarged prints were made

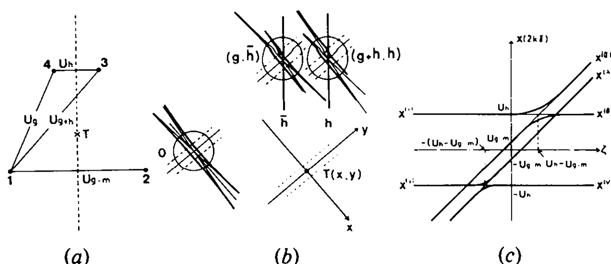

Fig. 1. Qualitative interpretation of the IKL method by four-beam approximation. (*a*) Reciprocal-lattice points, (*b*) schematic drawing of the IKL pattern and (*c*) dispersion surface.

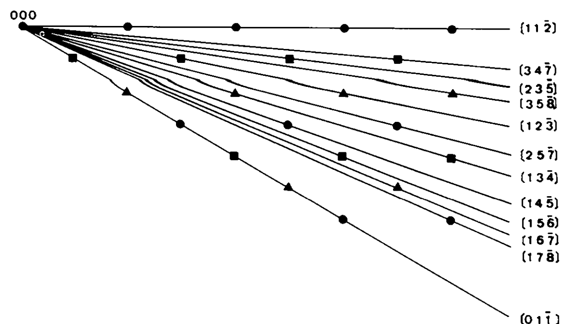

Fig. 2. Projections of reciprocal-lattice points along the [111] direction.

Table 1. *Separations of the Kikuchi-line segments, and f_{111}, f_{222}^{a} and f_{220} values corresponding to the stationary atom*

$(\mathbf{g}, \bar{\mathbf{h}})$	$(10\,0\,4, \bar{1}\bar{1}\bar{1})$ $(9\bar{1}3, \bar{2}\bar{2}\bar{2})$	$(9\bar{1}3, \bar{1}\bar{1}\bar{1})$ $(8\bar{2}2, \bar{2}\bar{2}\bar{2})$	$(0\,10\,6, \bar{1}\bar{1}\bar{1})$ $(\bar{1}95, \bar{2}\bar{2}\bar{2})$	$(95\bar{3}, \bar{2}\bar{2}0)$	Aldred & Hart (1973)
Separation (10^{-2} Å^{-1})	3·423 ± 0·052 3·561 ± 0·048	3·962 ± 0·048 3·999 ± 0·016	3·305 ± 0·024 3·165 ± 0·072	4·312 ± 0·005	
f_{111}	10·75 ± 0·05	10·71 ± 0·04	10·78 ± 0·05		10·739 ± 0·006
f_{222}^{a}	−0·41 ± 0·17	−0·28 ± 0·14	−0·04 ± 0·14		−0·177 ± 0·005
f_{220}				8·70 ± 0·01	8·651 ± 0·009

from each pattern on the gravure film instead of photographic paper, to avoid anisotropic expansion and contraction of the pattern. The measured separations are listed in Table 1. The accuracy was estimated to be 1–2%.

For determination of the 220 structure factor, the Kikuchi-line pattern of the $[3\bar{3}4]$ projection was selected (Fig. 4). Line segments at the intersections are much sharper than those in the $[23\bar{5}]$ projection, and the accuracy of measurement is higher, as can be seen in Table 1.

4. Calculations

For a diamond-type structure, the relation between U_h and the X-ray crystal structure factor without thermal vibration, F_h, is given by

$$U_h = \frac{m}{m_o}\frac{\exp[-B(\sin\theta/\lambda)^2]}{\pi V_c}\frac{2}{a_B}\frac{1}{(4\pi\sin\theta/\lambda)^2} \times (ZS_h - F_h), \qquad (6)$$

where a_B is the Bohr radius, S_h the geometrical structure factor, V_c the unit-cell volume, Z the atomic number, $\exp[-B(\sin\theta/\lambda)^2]$ the temperature factor, and the effect of anharmonicity is assumed to be negligible.

If the origin of the unit cell is taken at the bonding centre, the atoms have the fractional coordinates:

$$A: \tfrac{7}{8},\tfrac{7}{8},\tfrac{7}{8};\ \tfrac{3}{8},\tfrac{3}{8},\tfrac{7}{8};\ \tfrac{3}{8},\tfrac{7}{8},\tfrac{3}{8};\ \tfrac{7}{8},\tfrac{3}{8},\tfrac{3}{8};$$

$$B: \tfrac{1}{8},\tfrac{1}{8},\tfrac{1}{8};\ \tfrac{5}{8},\tfrac{5}{8},\tfrac{1}{8};\ \tfrac{5}{8},\tfrac{1}{8},\tfrac{5}{8};\ \tfrac{1}{8},\tfrac{5}{8},\tfrac{5}{8};$$

and S_{hkl} and F_{hkl} are given as

$$S_{hkl} = 8\cos\frac{\pi}{4}(h+k+l),$$

$$F_{hkl} = 8\left[f_h^{c,A}\cos\frac{\pi}{4}(h+k+l) + f_h^{a,A}\sin\frac{\pi}{4}(h+k+l)\right], \qquad (7)$$

where $f_h^{c,A}$ and $f_h^{a,A}$ are the centrosymmetric and anti-centrosymmetric parts of the scattering factor of atom A for reflexion $\mathbf{h}$. $f_h^{a,A}$ is expressed as

$$f_h^{a,A} = \frac{hkl}{(h^2+k^2+l^2)^{3/2}}\left\langle j_3\left(\frac{4\pi\sin\theta}{\lambda}r\right)\right\rangle, \qquad (8)$$

where $\langle j_3[(4\pi\sin\theta/\lambda)r]\rangle$ is the contribution of the radial part of the aspherical charge distribution (Dawson, 1967). Then, F_{111} and F_{222} are given by $-4\sqrt{2}(f_{111}^{c,A} - f_{111}^{a,A}) \equiv -4\sqrt{2}f_{111}$ and $-8f_{222}^{a,A} \equiv -8f_{222}^{a}$, respectively. If the origin is shifted to the anti-bonding centre, *i.e.* $\frac{1}{2},\frac{1}{2},\frac{1}{2}$, the sign of F_{111} will be

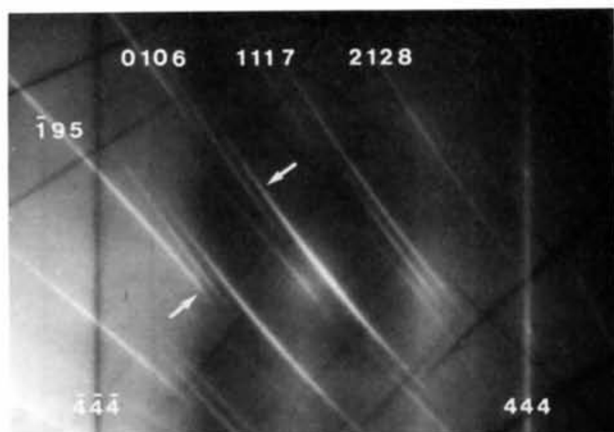

Fig. 3. Kikuchi-line pattern of Si ([235] projection, 1023 kV).

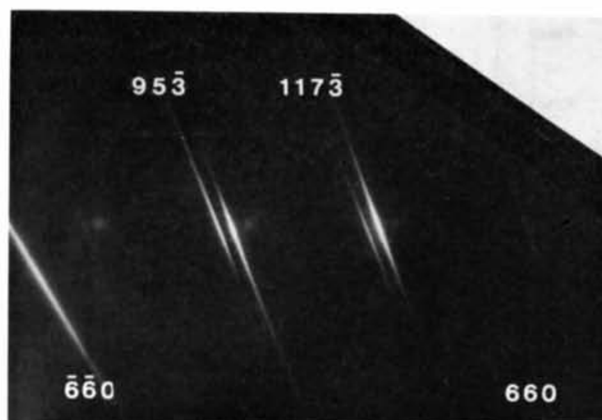

Fig. 4. Kikuchi-line pattern of Si ([3$\bar{3}$4] projection, 1023 kV).

reversed, whereas F_{222} is unchanged. In the present analyses, the origin is taken at the bonding centre. In the many-beam calculations for determining the 111, 222 and 220 structure factors, the atomic scattering factors given by Doyle & Turner (1968) were used for the higher-order structure factors, neglecting the anti-centrosymmetric part of the scattering factor due to the bonding effect. The B factor was assumed to be 0·46 Å^2.

Intensity profiles of the line segments were calculated from the slice formulation developed by Gjønnes (1966) and Høier (1972). With reasonable assumptions, the intensity in the $\mathbf{s} + \mathbf{h}$ direction for the crystal thickness t is given by

$$I_{s+h}(t) \sim \sum_j |C_o^{(j)} C_h^{(j)}|^2 \exp[-4\pi q^{(j)} t],$$
$$q^{(j)} = \frac{1}{2k} \sum_{g,g'} C_g^{(j)} U'_{g-g'} C_{g'}^{(j)}, \tag{9}$$

where the Bloch wave amplitude $C_h^{(j)}$ of the jth branch refers to the beam direction $\mathbf{k}_o + \mathbf{s}$ and $\mathbf{s}$ is taken to be a small vector within the first Brillouin zone, $q^{(j)}$ the absorption coefficient for the jth branch and U'_g the imaginary part of the structure factor. Let $T(x,y)$ be the projected centre of the Ewald sphere, in Fig. 1(b). The origin of the Cartesian coordinates (x,y) represents the kinematical simultaneous reflexion position for $\mathbf{g}$ and $\mathbf{g} + \mathbf{h}$, and the y axis is taken to be perpendicular to the line segments. For comparison with the measured separations, Kikuchi-line profiles were calculated along a series of y sections in the range $-0{\cdot}016 \le x \le 0{\cdot}016$ at intervals $\Delta x = 0{\cdot}004$ Å^{-1}.

The absorption causes a slight peak shift of the line segments in addition to the line broadening, since the two main branches contributing to each line segment have different absorption coefficients $q^{(j)}$ and give profiles, $|C_o^{(j)} C_h^{(j)}|^2 \exp[-4\pi q^{(j)} t]$, which are slightly different in peak positions. In order to estimate the effect of this on the separation, calculations were performed for four different crystal thicknesses, 0 (no absorption), 3000, 5000 and 7000 Å, using the g-dependent parameters U'_g/U_g for Si given by Humphreys & Hirsch (1968). The error in the separation of the line segments arising from the uncertainty of the crystal thickness was estimated to be 0·4% at most.

In order to find the number of interacting beams which are necessary for the many-beam calculations for determining the structure factors, the separation of the line segments was calculated as a function of the number of beams. The result obtained for the intersection ($9\bar{1}3$, $\bar{1}\bar{1}\bar{1}$) is shown in Fig. 5, where the f_{111} and f^a_{222} values have been assumed to be 10·7 and −0·15 respectively. It can be seen that eight systematic beams (group A in Fig. 5) are sufficient along the 111 row. The separation changes slightly when the beams of group B lying near the Ewald sphere are included, but it is sufficient if six such beams are taken into account. The beams of groups C and D have negligible effect on the separation, the effect of group C being counterbalanced by that of group D. In the calculations of the line separations, 19–24 beams were used.

Since both the f_{111} and f^a_{222} values are to be determined, only a functional relation between them is obtained from one separation. However, the intersecting point of two such relations obtained from the two separations at the intersections with the $\bar{1}\bar{1}\bar{1}$ and $\bar{2}\bar{2}\bar{2}$ lines gives both f_{111} and f^a_{222} values, as shown in Fig. 6, where the error limits shown by vertical lines were estimated from errors arising from measurements of separations and the uncertainty of the crystal thickness. The results obtained from three diffraction patterns are listed in Table 1, together with the X-ray data obtained by Aldred & Hart (1973) for comparison.

The value of f_{220}, on the other hand, can be determined uniquely from one separation. Since interactions

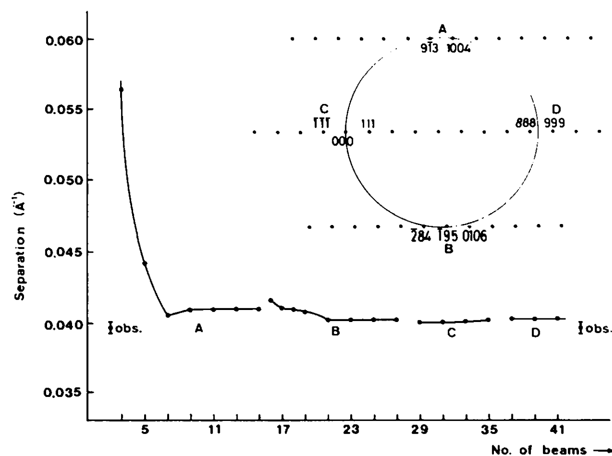

Fig. 5. Calculated separation of the line segments as a function of the number of interacting beams. Indices of the beams are shown in the inset.

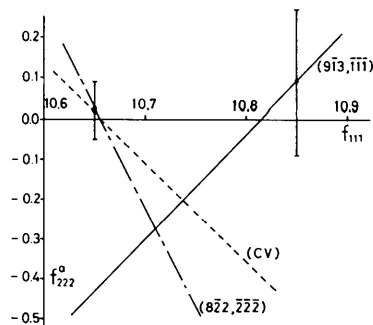

Fig. 6. Functional relations between f_{111} and f^a_{222} obtained for Si from the IKL experiment. The relation obtained by the critical-voltage method is also shown (broken line) for reference.

along the 220 systematic row are relatively weaker than those along the 111 row, the number of beams necessary for the calcualtions can be reduced. The result given in Table 1 was determined from the 16-beam calculation.

The present results agree well with the X-ray values, especially for the strong reflexions 111 and 220. The accuracy has been improved relative to measurements at 100 kV, particularly for 220 ($\pm 0 \cdot 4\%$ for U_{220}).

5. Discussion

Absolute measurements of the crystal structure factors of Si have been carried out with the X-ray *Pendellösung* method by many investigators, and the results obtained by Tanemura & Kato (1972) and Aldred & Hart (1973) are considered to be the most reliable and accurate. In their experiments, however, the weak 222 reflexion was not measured; f^a_{222} ($-0 \cdot 177$) listed in Table 1 is the value calculated from other structure factors based on Dawson's (1967) formalism. Recently, Fehlman & Fujimoto (1975) have performed the absolute X-ray measurement of the 222 structure factor and reported that $|F_{222}| = 1 \cdot 724 \pm 0 \cdot 036$ ($|f^a_{222}| = 0 \cdot 216 \pm 0 \cdot 004$).* However, the sign of the structure factor could not be determined directly by the X-ray method.

On the other hand, the sign can be determined, in principle, with electron diffraction methods based upon multiple-beam dynamical effects. Both the 111 and 222 structure factors of Si including the sign were determined by Kreutle & Meyer-Ehmsen (1971) from the measurement of rocking curves and by Ando, Ichimiya & Uyeda (1974) with the thickness fringe method. Smith & Lehmpfuhl (1975) also determined the structure factors by the convergent-beam electron diffraction method. The critical voltage for the 333 reflexion was measured by Hewat & Humphreys (1974) and Shishido & Tanaka (1975). However, since both the 111 and 222 structure factors cannot be determined simultaneously from one measured critical voltage, Hewat & Humphreys assumed the theoretical f^a_{222} value calculated by Aldred & Hart (1973) in the determination of the f_{111} value, and Shishido & Tanaka determined only a functional relation between them, which is shown in Fig. 6 (broken line) for reference. The 111 and 222 structure factors for X-rays reported by the authors mentioned above are listed in Table 2 together with those obtained in the present experiment. All the values have been readjusted for the stationary atom.

Table 2 shows that there is disagreement in the sign of F_{222}. However, the negative values of F_{222} reported in the previous electron diffraction studies can hardly be accepted for the following reasons: If we adopt the negative value of F_{222} and use the functional relation given by the critical-voltage method, an unreasonably small F_{111} value will be obtained, as can be understood from Fig. 6. Indeed, all three experimental relations shown in Fig. 6, *i.e.* the two intersections and the critical-voltage measurement, lead to a negative f^a_{222} value (= positive F_{222}) if Aldred & Hart's (1973) value for F_{111} is adopted. Furthermore, only a positive F_{222} appears consistent with the theoretical value of the covalent bonding charge, $\rho_{\text{valence}}(r)$ at $r = 0$. An

* This value was readjusted for the stationary atom, using a B factor of $0 \cdot 46$ Å^2.

Table 2. *Crystal structure factors of* Si *for X-rays obtained by the present method and those reported in the literature*

	$\|F_{111}\|$	F_{222}	$\|F_{220}\|$
Present			
$(10\bar{0}4, \bar{1}\bar{1}\bar{1})$ and $(9\bar{1}3, \bar{2}\bar{2}\bar{2})$	60·81 ± 0·28	3·28 ± 1·36	
$(9\bar{1}3, \bar{1}\bar{1}\bar{1})$ and $(8\bar{2}2, \bar{2}\bar{2}\bar{2})$	60·58 ± 0·23	2·24 ± 1·12	
$(0\,10\,6, \bar{1}\bar{1}\bar{1})$ and $(\bar{1}95, \bar{2}\bar{2}\bar{2})$	60·98 ± 0·28	0·32 ± 1·12	
$(95\bar{3}, \bar{2}\bar{2}0)$			69·60 ± 0·08
X-ray *Pendellösung*			
Tanemura & Kato (1972)	60·658 ± 0·012*		69·74 ± 0·01*
Aldred & Hart (1973)	60·726 ± 0·034†	1·42 ± 0·04	69·176 ± 0·072†
Fehlman & Fujimoto (1975)		1·724 ± 0·036‡	
Electron diffraction			
Kreutle & Meyer-Ehmsen (1971)	60·66 ± 0·05	−1·7 ± 0·2	
Hewat & Humphreys (1974)	60·590 ± 0·068		
Ando, Ichimiya & Uyeda (1974)	60·57 ± 0·47	−1·94 ± 0·89	
Smith & Lehmpfuhl (1975)	60·87 ± 0·10	−1·49 ± 0·42	

* Corrected for anomalous dispersion ($f' = 0 \cdot 06$).
† Corrected for nuclear Thomson scattering.
‡ Absolute value.

experimental value for $\rho_{\text{valence}}(0)$ can be obtained from the expression

$$\rho_{\text{valence}}(r) = \frac{1}{V_c} \sum \sum_{hkl} \sum (F_{hkl}^{\text{obs}} - F_{hkl}^{\text{core}}) \times \exp[-2\pi i(hx + ky + lz)], \quad (10)$$

where V_c is the volume of the unit cell, F_{hkl}^{obs} the observed structure factors and F_{hkl}^{core} the calculated structure factors for the core electrons of Si^{4+}. Using the structure factors determined by X-ray experiments and the F_{222} (1·416) calculated by Aldred & Hart (1973), Yang & Coppens (1974) obtained $\rho_{\text{valence}}(0) = 0{\cdot}67$ e Å^{-3}, in good agreement with the theoretical value, 0·65 e Å^{-3}, obtained by Walter & Cohen (1971) with the pseudopotential method. If a negative value is assumed for F_{222}, on the other hand, $\rho_{\text{valence}}(0)$ will be 0·55 e Å^{-3}, which is considerably smaller than the theoretical value. The negative sign of F_{222} in Table 2 can presumably be attributed to a lack of accuracy in the experiments or to some error in the conversion from the crystal potential V_{222} to the X-ray crystal structure factor F_{222}.

The present study shows that the accuracy of the crystal structure factor determination by the IKL method is improved by a factor of at least two on increasing the accelerating voltage from 100 to 1000 kV. The advantage of the method, that the determination of structure factors is relatively independent of other structure factors, can be maintained by a careful selection of the intersections. In the previous study of vanadium monoxide crystals at 100 kV (Høier & Andersson, 1974; Watanabe *et al.*, 1974), analyses were performed with the 19-beam calculations which are almost the same as in the present analysis.

In comparison with the critical-voltage method, the accuracy may still be poorer. On the other hand, structure factors which are not readily accessible to critical-voltage measurement can be determined, as in the present case where the sign and magnitude of F_{222} in silicon could be obtained with reasonable accuracy. Also, F_{220}, for which the critical voltage needed is well above 1000 kV (Arii & Uyeda, 1969), was determined. It is thus concluded that the IKL method represents a useful widening of possibilities for accurate structure factor determination from Kikuchi patterns.

The IKL patterns were obtained using a 1000 kV electron microscope in the High Voltage Electron Microscope Laboratory of Tohoku University. The authors wish to thank Mr H. Ohta for his help in the experiment. This work was partially supported by a Grant-in-Aid for Scientific Research from the Ministry of Education, Science and Culture.

References

ALDRED, P. J. E. & HART, M. (1973). *Proc. R. Soc. London Ser. A*, **332**, 223–238, 239–254.
ANDO, Y., ICHIMIYA, A. & UYEDA, R. (1974). *Acta Cryst.* A**30**, 600–601.
ARII, T. & UYEDA, R. (1969). *Jpn. J. Appl. Phys.* **8**, 621.
DAWSON, B. (1967). *Proc. R. Soc. London Ser. A*, **298**, 264–288.
DOYLE, P. A. & TURNER, P. S. (1968). *Acta Cryst.* A**24**, 390–397.
FEHLMAN, M. & FUJIMOTO, I. (1975). *J. Phys. Soc. Jpn*, **38**, 208–215.
FUKUHARA, A. (1966). *J. Phys. Soc. Jpn*, **21**, 2645–2662.
GJØNNES, J. (1966). *Acta Cryst.* **20**, 240–249.
GJØNNES, J. & HØIER, R. (1971). *Acta Cryst.* A**27**, 313–316.
GOODMAN, P. (1978). *Electron Diffraction* 1927–1977, edited by P. J. DOBSON, J. B. PENDRY & C. J. HUMPHREYS, pp. 116–128. Bristol and London: The Institute of Physics.
HEWAT, E. A. & HUMPHREYS, C. J. (1974). *High Voltage Electron Microscopy*, edited by P. R. SWANN, C. J. HUMPHREYS & M. J. GORINGE, pp. 52–56. New York and London: Academic Press.
HØIER, R. (1969). *Acta Cryst.* A**25**, 516–518.
HØIER, R. (1972). *Phys. Status Solidi A*, **11**, 597–610.
HØIER, R. & ANDERSSON, B. (1974). *Acta Cryst.* A**30**, 93–95.
HUMPHREYS, C. J. & HIRSCH, P. B. (1968). *Philos. Mag.* **18**, 115–122.
KREUTLE, M. & MEYER-EHMSEN, G. (1971). *Phys. Status Solidi A*, **8**, 111–118.
SHISHIDO, T. & TANAKA, M. (1975). *Jpn J. Appl. Phys.* **14**, 135–136.
SMITH, P. J. & LEHMPFUHL, G. (1975). *Acta Cryst.* A**31**, S220.
TANEMURA, S. & KATO, N. (1972). *Acta Cryst.* A**28**, 69–80.
WALTER, J. P. & COHEN, M. L. (1971). *Phys. Rev. B*, **4**, 1877–1892.
WATANABE, D., ANDERSSON, B., GJØNNES, J. & TERASAKI, O. (1974). *Acta Cryst.* A**30**, 772–776.
WATANABE, D., UYEDA, R. & FUKUHARA, A. (1968). *Acta Cryst.* A**24**, 580–581.
WATANABE, D., UYEDA, R. & FUKUHARA, A. (1969). *Acta Cryst.* A**25**, 138–140.
YANG, Y. W. & COPPENS, P. (1974). *Solid State Commun.* **15**, 1555–1559.